AIP | Applied Physics Letters

Dependence of inverse-spin Hall effect and spin-rectified voltage on tantalum thickness in Ta/CoFeB bilayer structure

Sang-Il Kim, Dong-Jun Kim, Min-Su Seo, Byong-Guk Park, and Seung-Young Park

Citation: Applied Physics Letters **106**, 032409 (2015); doi: 10.1063/1.4906487
View online: http://dx.doi.org/10.1063/1.4906487
View Table of Contents: http://scitation.aip.org/content/aip/journal/apl/106/3?ver=pdfcov
Published by the AIP Publishing

Articles you may be interested in

Stacking order dependence of inverse spin Hall effect and anomalous Hall effect in spin pumping experiments
J. Appl. Phys. **117**, 17D901 (2015); 10.1063/1.4906176

Strain-induced modulation of perpendicular magnetic anisotropy in Ta/CoFeB/MgO structures investigated by ferromagnetic resonance
Appl. Phys. Lett. **106**, 072402 (2015); 10.1063/1.4907677

Thickness dependence of spin torque ferromagnetic resonance in Co75Fe25/Pt bilayer films
Appl. Phys. Lett. **104**, 072405 (2014); 10.1063/1.4865425

Precessional magnetization induced spin current from CoFeB into Ta
Appl. Phys. Lett. **103**, 252409 (2013); 10.1063/1.4853195

Thickness dependence ferromagnetic resonance in Ta / Ni 81 Fe 19 bilayer nanostructures
AIP Conf. Proc. **1512**, 1172 (2013); 10.1063/1.4791466

This article is copyrighted as indicated in the article. Reuse of AIP content is subject to the terms at: http://scitation.aip.org/termsconditions. Downloaded to IP: 143.248.103.62 On: Thu, 02 Jul 2015 01:16:10

Dependence of inverse-spin Hall effect and spin-rectified voltage on tantalum thickness in Ta/CoFeB bilayer structure

Sang-Il Kim,[1] Dong-Jun Kim,[2] Min-Su Seo,[1] Byong-Guk Park,[2,a)] and Seung-Young Park[1,b)]
[1]*Division of Materials Science, Korea Basic Science Institute, Daejeon 305-806, South Korea*
[2]*Department of Materials Science and Engineering, KAIST, Daejeon 305-701, South Korea*

(Received 11 November 2014; accepted 11 January 2015; published online 21 January 2015)

Ta-layer thickness (t_{Ta}) dependence of the measured DC voltage V from the inverse-spin Hall effect (ISHE) in Ta/CoFeB bilayer structure is experimentally investigated using the ferromagnetic resonance in the TE_{011} resonant cavity. The ISHE signals excluding the spin-rectified effect (SRE) were separated from the fitted curve of V against t_{Ta}. For $t_{Ta} \approx \lambda_{Ta}$ (Ta-spin diffusion length = 2.7 nm), the deviation in ISHE voltage V_{ISH} between the experimental and theoretical values is significantly increased because of the large SRE contribution, which also results in a large deviation in the spin Hall angle θ_{SH} (from 10% to 40%). However, when $t_{Ta} \gg \lambda_{Ta}$, the V_{ISH} values are consistent with theoretical values because the SRE terms become negligible, which subsequently improves the accuracy of the obtained θ_{SH} within 4% deviation. The results will provide an outline for an accurate estimation of the θ_{SH} for materials with small λ value, which would be useful for utilizing the spin Hall effect in a 3-terminal spintronic devices in which magnetization can be controlled by in-plane current. © *2015 AIP Publishing LLC*.
[http://dx.doi.org/10.1063/1.4906487]

Pure spin current J_s, a flow of electron spins without charge current in a solid material, is of great importance in a research field of spintronics.[1] The generation of the J_s are mostly done by using a ferromagnet (FM) from which spin-polarized electrons are injected into an adjacent non-magnetic material (NM). There are various injection mechanisms proposed such as thermal spin injection,[2] direct electric spin injection,[3] and spin-pumping effect driven by ferromagnetic resonance (FMR).[4,5] Among them, the FMR spin-pumping is widely used to determine spin Hall angle θ_{SH} of the NM layer[6–8] because of better efficiency than others. Moreover, the spin injection by FMR spin pumping is free from the impedance mismatch problem.[9] The injected J_s in NM materials is converted into a charge current J_c via the inverse-spin Hall effect (ISHE) as[4]

$$J_c = \theta_{SH}\left(\frac{2e}{\hbar}\right) J_s \times \sigma, \tag{1}$$

where θ_{SH}, e, $\hbar$, and σ denote the spin Hall angle (the efficiency of spin-charge conversion), the elementary charge, the Dirac constant, and the spin-polarization vector of the J_s, respectively. Note that the θ_{SH}, which is related to spin-orbit interaction of the NM material, can be extracted from the measured ISHE voltage, V_{ISH} generated by the J_c. For example, the magnitude of the θ_{SH} is reported in the high-resistivity materials of β–Ta (−0.15)[10] and β–W (−0.3).[11] Note that a large and reliable θ_{SH} is very useful for optimizing the write impedance and minimizing the writing energy of a 3-terminal spin Hall effect device for achieving better performance and reliability in spin torque magnetic memory and spin logic applications, in comparison to conventional spin torque devices.[10]

The correct determination of the θ_{SH} is essential in order to employ the spin Hall effect in the spintronic devices. However, unfortunately, the measured DC voltage V from FMR spin-pumping experiment contains not only the V_{ISH} induced by pure spin pumping but also spin-rectified voltage V_{SR}. The latter results from the non-zero electric field from microwave (E_{MW}) which induced anisotropic magnetoresistance (AMR) and/or anomalous Hall effect (AHE) in the FM layer.[4,8,12–14] The non-negligible contribution of the V_{SR} (AMR voltage V_{AMR} and/or AHE voltage V_{AH}) hinders the correct estimation of the θ_{SH}, which may be the reason of the different reported θ_{SH} of nominally identical materials.[15,16] There are numerous studies[4,13,17,18] performed for decreasing the spin-rectified effect (SRE) to attain a more accurate θ_{SH} value. One of the examples is to place the samples at the center of a resonant cavity where the microwave magnetic field is maximized while the E_{MW} is minimized, which results in the suppression of the SRE contributions.[17] The other one is a selection of a proper microwave modes[18] in addition to the centering. A good understanding of these results is required for clarifying the origin of and correlation between ISHE and SRE in the bilayer structure.

In this study, the ISHE and the SRE in Ta (t_{Ta})/CoFeB (10 nm) bilayers were investigated as a function of the Ta-layer thickness (t_{Ta}) using FMR spin-pumping in the TE_{011} resonant cavity. When $t_{Ta} \gg \lambda_{Ta}$ (Ta-spin diffusion length = 2.7 nm),[16] the V_{ISH} values are consistent with theoretical values because the V_{SR} is negligible. Furthermore, the accuracy of θ_{SH} can be improved to within 4% deviation due to the reduced SRE. This indicates that the NM layer thickness for the FMR spin-pumping experiment to obtain the θ_{SH} should be appropriately chosen in the case of the NMs of small spin diffusion length λ, such as Ta.

Figure 1(a) shows schematic illustrations of the measurements of the FMR in the CoFeB single layer and of the

a)Email: bgpark@kaist.ac.kr
b)Email: parksy@kbsi.re.kr

 © 2015 AIP Publishing LLC

This article is copyrighted as indicated in the article. Reuse of AIP content is subject to the terms at: http://scitation.aip.org/termsconditions. Downloaded to IP: 143.248.103.62 On: Thu, 02 Jul 2015 01:16:10

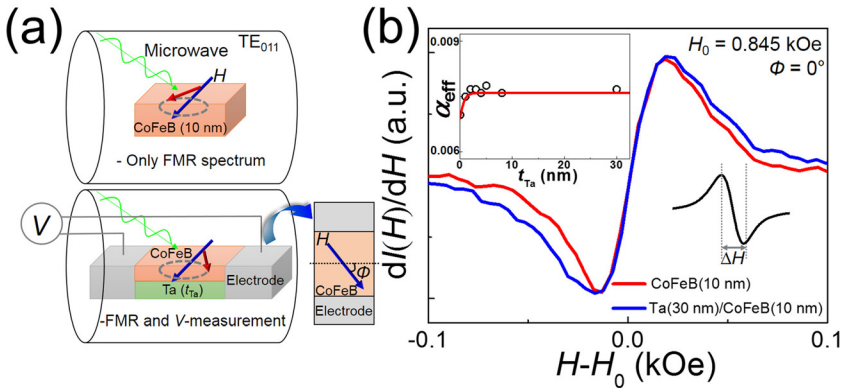

FIG. 1. (a) Schematic illustrations of the measurements of the samples (CoFeB single layer and Ta/CoFeB bilayer) in the TE_{011} resonant cavity. Here, the samples are placed near the center of the resonant cavity to minimize the spin-rectified effect (SRE). The external magnetic field H is applied along the sample plane. ϕ is the in-plane angle between H and transverse axis. (b) The H dependence of the ferromagnetic resonance for the CoFeB (10 nm) single layer and Ta (30 nm)/CoFeB (10 nm) bilayer. Here, I, ΔH, and H_0 ($=0.845$ kOe) denote the microwave absorption intensity, the spectral width, and the resonance magnetic field, respectively. The inset shows the t_{Ta} dependence of α_{eff} (the effective Gilbert damping constant) estimated from the ferromagnetic resonance results obtained for the CoFeB single layer and Ta/CoFeB bilayer samples.

FMR and V in the Ta/CoFeB bilayer. The bilayer samples of a 10-nm-thick FM CoFeB layer and a Ta layer of thickness $t_{Ta}=1$–30 nm were sputtered on thermally oxidized Si substrates. The dimension of the samples is 1 mm (width) × 2 mm (length). In order to measure V, two electrodes are kept in contact with both ends of the bilayer sample (the sign of V is determined by the measurement conditions and is considered to be positive for the present measurements). In accordance with the previous studies,[18] the present experiments minimize the effect of E_{MW} by optimizing the DUT (device under test) centering; the DUT is placed near the center of a TE_{011} cylindrical cavity.

Note that the typical spin-pumping method with a coplanar wave-guide (CPW) shows a superimposed signal of V_{ISH} and V_{SR},[8] because of non-zero angle (φ) between applied field (H) and longitudinal axis of the sample, with a relation of the ISHE ($\propto \sin(\varphi)$) and AMR ($\propto \sin(\varphi)\cos(\varphi)$). On the other hand, the cavity method has provided more convenient way to separate AMR ($V_{AMR}\sin(2\phi)\sin(\phi)$) and ISHE ($V_{ISH}\cos(\phi)$) signal, since the ϕ can be zero.[13] Here, the ϕ ($=90^\circ-\varphi$) is the in-plane angle between H and transverse axis. Therefore, the cavity method has an angle (ϕ) depending AMR free environment when ϕ is zero, and finally, the V_{ISH} shows a clear dependence of the t_{Ta}.

Figure 1(b) shows the measured FMR as a function of H for the CoFeB single layer and the Ta (30 nm)/CoFeB (10 nm) bilayer. Here, the microwave frequency is 9.46 GHz, microwave power is 50 mW, and resonance field H_0 is 0.845 kOe. In the FMR data, I denotes the microwave absorption intensity. The full width at half maximum of $I(H)$, ΔH ($=4\pi f_0\alpha_{eff}/\sqrt{3}\gamma$), shown in the inset), for the CoFeB is enlarged by attaching the Ta layer, where f_0, α_{eff}, and γ are the resonance frequency, effective Gilbert damping constant, and gyromagnetic ratio, respectively. The α_{eff} is determined by modification of the intrinsic damping constant, α_0, of CoFeB by additional damping ($\Delta\alpha$) from the spin pumping effect. The increase in the damping constant demonstrates an evidence of the J_s injection using FMR spin-pumping. The inset shows the t_{Ta} dependence of the α_{eff} (symbols) extracted from ΔH. Here, the α_{eff} for the Ta/CoFeB bilayer is given by[19]

$$\alpha_{eff}(t_{Ta}) \approx \alpha_0 + \frac{A_1}{1+\left(2\sqrt{(Z_{Ta}\alpha_{fs})^4/3}\tanh(t_{Ta}/\lambda_{Ta})\right)^{-1}}, \quad (2)$$

where Z_{Ta} and α_{fs} are the atomic number of Ta and fine-structure constant, respectively. The parameter A_1 ($=g\mu_B g^{\uparrow\downarrow}/4\pi M_s t_{CoFeB}$) is a constant for Ta/CoFeB structures which involves the g-factor, the Bohr magneton μ_B, the saturation magnetization M_s, thickness of CoFeB layer t_{CoFeB}, and the spin mixing conductance $g^{\uparrow\downarrow}$. The red curve shows a fitting to Eq. (2) with $\lambda_{Ta}=2.7$ nm, $A_1=0.002$, and $\alpha_0=0.007$ (y-intercept). The value of α_0 for the CoFeB single layer agrees reasonably with previous experimental results.[18] The reported $\alpha_0=0.015$ for a 5-nm CoFeB single layer is twice that a 10 nm CoFeB, thus $\alpha_0 \propto t_{CoFeB}{}^{-1}$.[20,21] α_{eff} is initially increased with t_{Ta} up to the λ_{Ta} and no variation at larger t_{Ta}. This indicates that the J_s value at the Ta/CoFeB interface is suppressed at smaller t_{Ta} due to the backflow of the J_s, which can be neglected for larger t_{Ta} than the λ_{Ta}. These results are also consistent with the previous experimental data for α_{eff} with respect to the thickness of the NM layer.[19]

Figures 2(a) and 2(b) show the H dependence of V measured for the Ta (t_{Ta})/CoFeB (10 nm) bilayer samples under the FMR condition. In the $t_{Ta}<\lambda_{Ta}$ region (shown in Figure 2(a)), the amplitude of $V(H)$ is increased with t_{Ta}. Furthermore, the antisymmetric component is clearly observed in the $V(H)$ curve, which can be attributed to the undesired SRE signal. In other words, the $V(H)$ is given by the sum of the two contributions: ISHE and SRE, which have different symmetry with respect to the resonance magnetic field. The voltage from the ISHE typically shows a symmetric curve that can be expressed by a Lorentzian curve, while that from the SRE does an antisymmetric dispersive curve. On the other hand, in the $t_{Ta}>\lambda_{Ta}$ region (shown in Figure 2(b)), the amplitude of $V(H)$ shows a monotonic decrease with the increase in t_{Ta} and the shape of $V(H)$ curves become more symmetric. Next, in order to extract the ISHE and SRE components from the experimental $V(H)$ curves, the $V(H)$ data were analyzed by fitting into a simple function consisted of the V_{ISH} and the V_{SR}.

This article is copyrighted as indicated in the article. Reuse of AIP content is subject to the terms at: http://scitation.aip.org/termsconditions. Downloaded to IP: 143.248.103.62 On: Thu, 02 Jul 2015 01:16:10

Figure 3(a) shows the theoretical fits of the experimental $V(H)$ data (Figure 2) obtained from the Ta (t_{Ta})/CoFeB (10 nm) bilayer with t_{Ta} varying from 1 nm to 30 nm. The measured $V(H)$ signals under the FMR condition are well-fitted using the following function[18]

$$V(H) = V_{ISHE}(H) + V_{SRE}(H) = V_{ISH}\frac{\Delta H^2}{(H-H_0)^2+\Delta H^2} + V_{SR}\frac{-2\Delta H(H-H_0)}{(H-H_0)^2+\Delta H^2}, \quad (3)$$

where the first and second terms indicate the ISHE and SRE contributions, respectively. The terms of $V_{ISHE}(H)$ and the $V_{SRE}(H)$ are proportional to the inverse-spin Hall coefficient of Ta and the spin rectification coefficient of CoFeB, respectively. It is worth noting that the shapes of the $V(H)$ curves are dependent on t_{Ta}. The $V(H)$ curve becomes symmetric on increasing t_{Ta}.

Figure 3(b) presents the t_{Ta} dependence of the V_{ISH} (magnitude of $V_{ISHE}(H)$) and V_{SR} (magnitude of $V_{SRE}(H)$) extracted from the fitted $V(H)$ curves, which is shown in Figure 3(a). V_{ISH} (red open squares) is designated as the peak height of the Lorentzian function. As is well known, V_{ISH} for the bilayer system is theoretically given by[19]

$$V_{ISH}(t_{Ta}) \approx \frac{c_1\theta_{SH}\tanh(t_{Ta}/2\lambda_{Ta})\left(1+\left(2\sqrt{(Z_{Ta}\alpha_{fs})^4/3}\tanh(t_{Ta}/\lambda_{Ta})\right)^{-1}\right)^{-1}}{(1+(\rho_{CoFeB}/\rho_{Ta}t_{CoFeB})t_{Ta})\left(\alpha_0+A_1\left(1+\left(2\sqrt{(Z_{Ta}\alpha_{fs})^4/3}\tanh(t_{Ta}/\lambda_{Ta})\right)^{-1}\right)^{-1}\right)^2}, \quad (4)$$

where ρ_{CoFeB} is the resistivity of CoFeB and ρ_{Ta} is the resistivity of Ta. The parameter c_1 involves physical constants such as the initial J_s value at the Ta/CoFeB interface J_s^0, f_0, γ, M_s, and the microwave magnetic field h_{rf}. The magenta line in the Figure 3(b) is the best fit to the V_{ISH} data obtained with Eq. (4) and reasonable material parameters. The experimentally measured parameters are $\alpha_0 \approx 0.007$, $A_1 \approx 0.002$, $\rho_{Ta} \approx 210\,\mu\Omega\cdot$cm, and $\rho_{CoFeB} \approx 180\,\mu\Omega\cdot$cm, and the well-fitting parameters are $\lambda_{Ta} = 2.5 \pm 0.5$ nm (the deviation originates from the quality of the thin film) and $c_1 = 0.03 \pm 0.01\,\mu$V (the calculated $h_{rf} \approx 1$ Oe). The parameters are comparable to previous experimental data for V_{ISH} vs. the thickness of a Pt layer (with a fixed FM layer).[19] The V_{ISH} values show a monotonic decrease with the increase in t_{Ta} for $t_{Ta} > \lambda_{Ta}$. According to a simple circuit model, this originates from the reduction in the resistance of Ta, R_{Ta} ($= \rho_{Ta}l/(wt_{Ta})$, where l (w) is a length (width) of the sample). This is because the measured voltage is described as $1/V_{ISH} = 1/(R_{Ta}\,I_c) + 1/(R_{CoFeB}\,I_c)$, where R_{CoFeB} and I_c are the resistance of the CoFeB layer and the induced current from spin pumping. On the contrary, in the $t_{Ta} < \lambda_{Ta}$ region, the V_{ISH} values are decreased with decreasing t_{Ta} because J_s^o generated by the spin-pumping effect is decreased owing to the backflow of J_s, which is related to the variation of α_{eff} (see the inset of Figure 1(b)). To analyze the contribution of SRE in the bilayer according to t_{Ta}, the NM/FM bilayer is assumed to be two independent resistors (R_{CoFeB} or R_{Ta}) connected in parallel; this is called the two-channel model. In this model, it can be also assumed that the spin-rectified voltage is generated only by the CoFeB layer. The total induced current I_{total} and voltage V_{total} in the sample can be expressed as $I_{total} = I_{CoFeB} + I_{Ta}$ and $V_{total} = R_{CoFeB}\,I_{CoFeB} = R_{Ta}\,I_{Ta}$, where the subscripts indicate the CoFeB and Ta layers, respectively. Therefore, the V_{SR} as a function of the t_{Ta} can be expressed as[22]

$$V_{SR}(t_{Ta}) \approx \frac{C_{SRE}(\propto \rho_{SR})}{(\rho_{CoFeB}/\rho_{Ta}t_{CoFeB})t_{Ta}+1}, \quad (5)$$

where ρ_{SR} is resistivity corresponded to the spin-rectification in the bilayer. The cyan line in Figure 3(b) is the best fit to the V_{SR} data obtained with Eq. (5), $C_{SRE} \approx 22\,\mu$V, and the above-mentioned parameters (ρ_{CoFeB}, ρ_{Ta}, t_{CoFeB}). The experimental V_{SR} values in the bilayer system are consistent

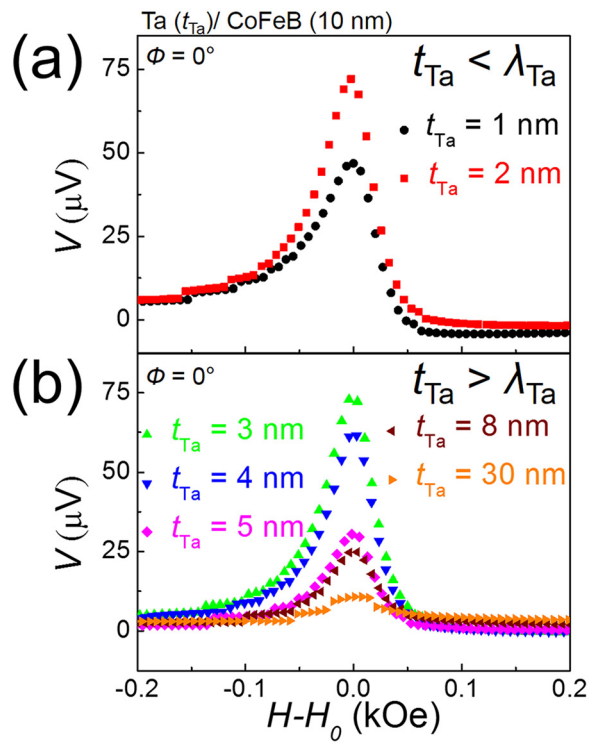

FIG. 2. H dependence of V for Ta (t_{Ta})/CoFeB (10 nm) bilayer samples. The experimental curves of V are divided on the basis of the Ta-spin diffusion length λ_{Ta} ($= 2.7$ nm) as (a) $t_{Ta} < \lambda_{Ta}$ and (b) $t_{Ta} > \lambda_{Ta}$.

This article is copyrighted as indicated in the article. Reuse of AIP content is subject to the terms at: http://scitation.aip.org/termsconditions. Downloaded to IP: 143.248.103.62 On: Thu, 02 Jul 2015 01:16:10

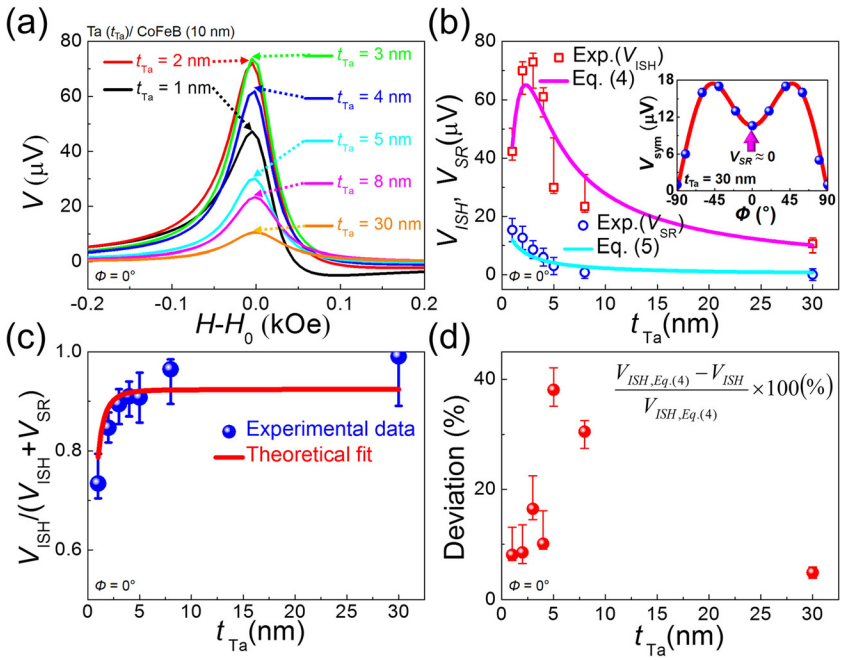

FIG. 3. (a) The fitting results from the experimental $V(H)$ data (in Figure 2). (b) The t_{Ta} dependence of V_{ISH} (open squares) and V_{SR} (open circles). The data points are taken from Figure 3(a). The solid magenta line shows the fitting result for the V_{ISH} data. The solid cyan line shows the fitting result for the V_{SR} data. Inset shows the dependence of the V_{sym} as a function of ϕ. (c) The t_{Ta} dependence of $V_{ISH}/(V_{ISH}+V_{SR})$ ratios. The red curve shows the theoretical fit. (d) The t_{Ta} dependence of deviation (%) between the theoretical and the experimental V_{ISH} values is shown.

with the theoretical values (from Eq. (5)) based on the two-channel model. Note that the V_{SR} values are especially increased with decreasing t_{Ta}. The inset in Figure 3(b) shows data for the symmetric component of $V(H,\phi)$ ($= V_{sym}$) fitted by Eq. (3) for fixed $t_{Ta} = 30$ nm and varying ϕ. The solid line in the inset of Figure 3(b) is the well fit to the experimental data using $V_{sym}(\phi) = V_{ISH}(= 10.6\,\mu V)\cos(\phi) + V_{AMR}(= 13.8\,\mu V)\sin(2\phi)\sin(\phi)$, according to Ref. 13. From this result, the SRE contribution to the $V(H,\phi)$ in the resonant cavity system is practically negligible at the $t_{Ta} \gg \lambda_{Ta}$ and $\phi = 0°$.

The relative magnitude of the ISHE expressed by $V_{ISH}/(V_{ISH}+V_{SR})$, as shown in Figure 3(c), is initially increased and saturated with an increase of the t_{Ta}, which is due to the reduction of SRE. The red curve shows $V_{ISH}/(V_{ISH}+V_{SR})$ vs. t_{Ta} estimated from Eqs. (4) and (5). These results indicate that the SRE contribution is practically negligible for $t_{Ta} \gg \lambda_{Ta}$. With this reason, in the $t_{Ta} < \lambda_{Ta}$ region where the SRE is relatively large, the deviation in V_{ISH} values between the theoretical (Eq. (4)), and experimental data are also increased by 10%–40% (Figure 3(d); the deviation is defined by $(V_{ISH,\ Eq.\ (4)} - V_{ISH,\ experimental\ data}/V_{ISH,\ Eq.\ (4)} \times 100)$. However, when t_{Ta} is sufficiently large where the SRE is negligible, the deviation in V_{ISH} can be decreased to within 4%.

Formerly, the measurement of $V(H)$ is focused on sample geometry (length, width, and thickness dimensions), which is determined to obtain a highly suitable V_{ISH} value.[19] It was reported that the magnitude of V_{ISH} is proportional to the length of the bilayer sample and does not vary on the width of the bilayer sample.[23] Moreover, the V_{ISH} attains its maximum value when the thickness of the NM layer in the NM/FM bilayer is close to the λ of the NM material.[19] Unfortunately, for materials with a small λ such as Ta, the maximum V_{ISH} value (assuming $t_{Ta} \approx \lambda_{Ta}$) showed a large deviation from the model calculation due to the large SRE contribution, regardless of the resistivity of each layer (CoFeB and Ta). Consequently, the θ_{SH} obtained from the V_{ISH} also shows a discrepancy with a theoretical θ_{SH} value for the Ta material calculated from Eq. (4) with the above-mentioned parameters ρ_{Ta}, ρ_{CoFeB}, c_1, α_0, λ_{Ta}, and V_{ISH}. When t_{Ta} ($=3$ nm) $\approx \lambda_{Ta}$, the obtained θ_{SH} value for Ta with an experimental value of $V_{ISH} = 69 \pm 8\,\mu V$ is 0.025 ± 0.008 (the deviation originates from the SRE). However, when t_{Ta} ($= 30$ nm) $\gg \lambda_{Ta}$, the θ_{SH} value for Ta with $V_{ISH} = 9.8 \pm 2.8\,\mu V$ is 0.02 ± 0.0007. There have been several discrepancies in the values of θ_{SH} reported in the literature,[15] which could be explained by the fact that the antisymmetric component of V_{SR} is not appropriately considered when measuring V_{ISH} in the bilayer structure.[24] It is important that the θ_{SH} value for Ta can be obtained with high accuracy at $t_{Ta} \gg \lambda_{Ta}$ by eliminating the SRE contribution in the V_{ISH} measurement.

In summary, the t_{Ta} dependences of the spin pumping voltage $V(H,\phi)$ (from ISHE and SRE) in Ta (t_{Ta})/CoFeB bilayers were experimentally investigated using the FMR in the TE_{011} resonant cavity. The ISHE signals are well separated from the fitted curve of $V(H,\phi)$ against t_{Ta}. For $t_{Ta} \approx \lambda_{Ta}$, the deviation in V_{ISH} values between the experimental and theoretical values are increased with decreasing t_{Ta} because of the large SRE contribution, which also increases the deviation in the θ_{SH} value for Ta from 10% to 40% (0.025 ± 0.008). However, when $t_{Ta} \gg \lambda_{Ta}$, the V_{ISH} values are consistent with theoretical values because of the negligible SRE (with increasing t_{Ta}). Furthermore, the accuracy of θ_{SH} is improved with reduced SRE to $\theta_{SH} = 0.02 \pm 0.0007$ (within 4% deviation). These results will provide an outline for accurately estimating the θ_{SH} parameter for materials with a large θ_{SH} value and a small λ value.

This research was supported by the Pioneer Research Center Program through the National Research Foundation of Korea funded by the Ministry of Science, ICT & Future Planning (2011-0027908); by a grant from the R&D Program for Industrial Core Technology funded by the Ministry of Trade, Industry and Energy (MOTIE), Republic

This article is copyrighted as indicated in the article. Reuse of AIP content is subject to the terms at: http://scitation.aip.org/termsconditions. Downloaded to IP: 143.248.103.62 On: Thu, 02 Jul 2015 01:16:10

of South Korea (Grant No. 10044723); and by National Research Foundation Grant (NRF-2012R1A1A1041590) funded by the Ministry of Science, ICT & Future Planning.

[1]S. A. Wolf, D. D. Awschalom, R. A. Buhrman, J. M. Daughton, S. von Molnar, M. L. Roukes, A. Y. Chtchelkanova, and D. M. Treger, Science **294**, 1488 (2001).
[2]K. Uchida, M. Ishida, T. Kikkawa, A. Kirihara, T. Murakami, and E. Saitoh, J. Phys.: Condens. Matter **26**, 343202 (2014).
[3]F. J. Jedema, A. T. Filip, and B. J. van Wees, Nature (London) **410**, 345 (2001).
[4]E. Saitoh, M. Ueda, H. Miyajima, and G. Tatara, Appl. Phys. Lett. **88**, 182509 (2006).
[5]S. R. Boona, R. C. Myers, and J. P. Heremans, Energy Environ. Sci. **7**, 885 (2014).
[6]C. Hahn, G. de Loubens, O. Klein, M. Viret, V. V. Naletov, and J. Ben Youssef, Phys. Rev. B **87**, 174417 (2013).
[7]H. L. Wang, C. H. Du, Y. Pu, R. Adur, P. C. Hammel, and F. Y. Yang, Phys. Rev. Lett. **112**, 197201 (2014).
[8]O. Mosendz, V. Vlaminck, J. E. Pearson, F. Y. Fradin, G. E. W. Bauer, S. D. Bader, and A. Hoffmann, Phys. Rev. B **82**, 214403 (2010).
[9]K. Ando, S. Takahashi, J. Ieda, H. Kurebayashi, T. Trypiniotis, C. H. W. Barnes, S. Maekawa, and E. Saitoh, Nat. Mater. **10**, 655 (2011).
[10]L. Q. Liu, C. F. Pai, Y. Li, H. W. Tseng, D. C. Ralph, and R. A. Buhrman, Science **336**, 555 (2012).
[11]C.-F. Pai, L. Liu, Y. Li, H. W. Tseng, D. C. Ralph, and R. A. Buhrman, Appl. Phys. Lett. **101**, 122404 (2012).
[12]K. Ando, S. Takahashi, J. Ieda, Y. Kajiwara, H. Nakayama, T. Yoshino, K. Harii, Y. Fujikawa, M. Matsuo, S. Maekawa, and E. Saitoh, J. Appl. Phys. **109**, 103913 (2011).
[13]A. Azevedo, L. H. Vilela Leão, R. L. Rodríguez-Suárez, A. F. Lacerda Santos, and S. M. Rezende, Phys. Rev. B **83**, 144402 (2011).
[14]W. Zhang, V. Vlaminck, J. E. Pearson, R. Divan, S. D. Bader, and A. Hoffmann, Appl. Phys. Lett. **103**, 242414 (2013).
[15]A. Hoffmann, IEEE Trans. Magn. **49**, 5172 (2013).
[16]M. Morota, Y. Niimi, K. Ohnishi, D. H. Wei, T. Tanaka, H. Kontani, T. Kimura, and Y. Otani, Phys. Rev. B **83**, 174405 (2011).
[17]K. Harii, K. Ando, H. Y. Inoue, K. Sasage, and E. Saitoh, J. Appl. Phys. **103**, 07F311 (2008).
[18]S.-I. Kim, M.-S. Seo, and S.-Y. Park, J. Appl. Phys. **115**, 17C501 (2014).
[19]H. Nakayama, K. Ando, K. Harii, T. Yoshino, R. Takahashi, Y. Kajiwara, K. Uchida, Y. Fujikawa, and E. Saitoh, Phys. Rev. B **85**, 144408 (2012).
[20]E. Barati, M. Cinal, D. M. Edwards, and A. Umerski, EPJ Web Conf. **40**, 18003 (2013).
[21]X. Liu, W. Zhang, M. J. Carter, and G. Xiao, J. Appl. Phys. **110**, 033910 (2011).
[22]W. J. Xu, B. Zhang, Z. Wang, S. S. Chu, W. Li, Z. B. Wu, R. H. Yu, and X. X. Zhang, Eur. Phys. J. B **65**, 233 (2008).
[23]H. Nakayama, K. Ando, K. Harii, Y. Fujikawa, Y. Kajiwara, T. Yoshino, and E. Saitoh, J. Phys.: Conf. Ser. **266**, 012100 (2011).
[24]D.-J. Kim, S.-I. Kim, S.-Y. Park, K.-D. Lee, and B.-G. Park, Curr. Appl. Phys. **14**, 1344 (2014).

This article is copyrighted as indicated in the article. Reuse of AIP content is subject to the terms at: http://scitation.aip.org/termsconditions. Downloaded to IP: 143.248.103.62 On: Thu, 02 Jul 2015 01:16:10